Leu505 of neutrophil Nox2 is crucial in the NADPH-binding process during NADPH oxidase activation

Xing Jun Li[*], Franck Fieschi†, Marie-Hélène Paclet[*], Didier Grunwald‡, Yannick Campion[*], Philippe Gaudin[*], Françoise Morel[*] and Marie-José Stasia[*]

From the [*]Groupe de Recherche et d'Etude du Processus Inflammatoire EA 2938 Université Joseph Fourier, Laboratoire d'Enzymologie, Centre Hospitalier Universitaire, 38043 Grenoble Cedex 9, the † Institut de Biologie Structurale, UMR 5075 CEA/CNRS/Université Joseph Fourier, Laboratoire des Proteines Membranaires, 41 rue Jules Horowitz 38027 Grenoble cedex 1, and the ‡Département Réponse et Dynamique Cellulaire/Commissariat à l'Energie Atomique, 17 rue des Martyrs, 38054 Grenoble Cedex 9, France.

Name and address of corresponding author:

Name Marie-José Stasia

Address GREPI, EA UJF laboratoire d'Enzymologie, CHU
38043 Grenoble Cedex 9, France

Telephone 33 (0)4 76 76 54 83

Fax 33 (0)4 76 76 56 08

E-mail MJStasia@chu-grenoble.fr

Key words: NADPH oxidase, activation, NADPH binding, α-helical loop, cytosolic C-terminal tail, Nox2

ABSTRACT

The role of Leu^{505} of Nox2 on NADPH oxidase activation process was investigated. An X-CGD PLB-985 cell line expressing Leu505Arg Nox2 mutant was obtained, exactly mimicking the phenotype of a previously published $X91^{+}$-CGD case. While the NADPH oxidase activity of mutant transfected cells was abolished, translocation of $p67^{phox}$ and $p47^{phox}$ to the plasma membrane occurred normally. In a reconstituted cell-free system (CFS), NADPH oxidase and iodonitrotetrazolium (INT) reductase activities were partially maintained, suggesting that assembly and electron transfer from NADPH could take place in the Leu505Arg Nox2 mutant. However, in a simplified CFS using purified mutant cytochrome b_{558} and recombinant $p67^{phox}$, $p47^{phox}$ and Rac1proteins, we found that the K_m for NADPH and for NADH was about three times higher than those of purified WT cytochrome b_{558}, indicating that Leu505Arg mutation slightly decreases the affinity for NADPH and NADH. In addition, oxidase activity can be extended by increasing the amount of $p67^{phox}$ in the simplified CFS assay. However, the maximal reconstituted oxidase activity using WT purified cytochrome b_{558} could not be reached using mutant cytochrome b_{558}. In a three-dimensional model of the C-terminal tail of Nox2, Leu^{505} appears to have a strategic position just at the entry of the NADPH binding site and at the end of the α-helical loop (residues 484–504), a potential binding region of cytosolic factors. Leu505Arg mutation could alter the α-helical loop position, thus affecting NADPH access to its binding site. However, Leu^{505} seems not to be directly involved in the binding of NADPH.

INTRODUCTION

Professional phagocytes generate high levels of reactive oxygen species (ROS) by activating a superoxide-generating NADPH oxidase, one of the crucial elements of microbicidal mechanisms. The NADPH oxidase is a multi-component enzyme composed of a membrane-associated flavocytochrome b_{558} and cytosolic proteins $p67^{phox}$, $p47^{phox}$, $p40^{phox}$ and Rac [1-2]. Flavocytochrome b_{558}, the catalytic center of the NADPH oxidase, consists of a heavily glycosylated large β-subunit ($gp91^{phox}$, Nox2) and a small α subunit ($p22^{phox}$). In resting cells, $p67^{phox}$, $p40^{phox}$ and/or $p47^{phox}$ form a cytosolic complex dissociated with cytochrome b_{558} [3-4]. In resting neutrophils, this oxidase is inactive in a dissociated state and becomes assembled and activated by exposure to microorganisms or inflammatory mediators. Indeed, upon activation, $p47^{phox}$ is highly phosphorylated and mediates $p67^{phox}$ and/or $p40^{phox}$ translocation to the plasma membrane as an organizer. $P67^{phox}$, which is essential for oxidase activation, serves as an activator. However, the small GTP-binding protein Rac (Rac1/2) translocates independently of the other cytosolic components [5]. $P22^{phox}$ seems to play a docking site role for the cytosolic oxidase components and especially for $p47^{phox}$ [6-7], while Nox2 is the only catalytic element of the NADPH oxidase complex. It contains six α-helix transmembrane domains in the N-terminus in which two hemes [8] and the glycosylation sites are localized [9].

The C-terminus of Nox2 is a cytosolic sequence supporting the NADPH and FAD binding sites. Based on sequence alignments of $gp91^{phox}$ with flavoproteins and reductases, two regions, ^{338}HPFTLTSA^{345} and ^{355}IRIVGD^{360}, are proposed as binding sites for FAD. In addition, four cytosolic sequences, namely ^{405}MLVGAGIGVTPF^{416}, ^{442}YWLCRD^{447}, ^{504}GLKQ^{507} and ^{535}FLCGPE^{540}, are considered to be binding sites for pyrophosphate, ribose, adenine and the nicotinamide unit of NADPH, respectively [10-12]. In the predicted three-dimensional structure model of Nox2, another intriguing sequence composed of residues 484–504 and localized near the potential adenine of the NADPH binding site has been proposed to form an α-helical loop covering the cleft in which NADPH binds in the inactive state of the enzyme [13]. Upon oxidase activation, access of NADPH to the binding site could potentially be regulated by the interaction of this loop with oxidase cytosolic factors. This α-helical loop is specifically found in the Nox-Duox family and ferric reductase (FRE1) but not in other FNR reductases [13].

Chronic granulomatous disease (CGD), a rare congenital disorder in which the phagocytic cells fail to generate superoxide (O_2^-) and characterized by severe recurrent bacterial and fungal infections,

results from mutations in one of the four subunits of NADPH oxidase [14-16]. $X91^{+}$-CGD cases, characterized by normal expression of a nonfunctional Nox2 protein, are rare and useful CGD variants to study functional domains of Nox2. Indeed, the missense mutations Gly408Glu and Asp500Gly, located in the pyrophosphate-binding site for NADPH and in the C-terminal α-helical loop, respectively, disturb the NADPH oxidase assembly and electron transfer [17-18]. This suggests that an intimate relation exists between the electron transfer and the oxidase assembly processes in certain Nox2 domains. In addition, in transgenic X-CGD PLB-985 cell models, we demonstrated that point mutations in Asp^{484} and Asp^{500}, located in the α-helical loop, were essential to the oxidase assembly and to maintaining the electron transfer from NADPH to FAD [19]. Recently, Stasia *et al.* [20] have reported a new $X91^{+}$-CGD case characterized by a missense mutation Leu505Arg in the potential NADPH-binding site of Nox2 close to the predicted cytosolic C-terminal α-helical loop.

In this study, transfected PLB-985 cells mimicking the previously reported $X91^{+}$-CGD case were used to elucidate the impact of Leu505Arg mutation on NADPH oxidase activation. Purified Leu505Arg mutant and wild-type (WT) cytochrome b_{558} purified from transfected PLB-985 cells were used in a simplified cell-free system (CFS) with recombinant proteins $p67^{phox}$, $p47^{phox}$ and Rac1 to study the effect of increasing the amount of NADPH and $p67^{phox}$ on NADPH oxidase activity. The three-dimensional model of the C-terminal tail of Nox2 was used to determine the strategic importance of the Leu^{505} position on the NADPH oxidase activation process.

EXPERIMENTAL PROCEDURE

Materials

Diisopropylfluorophosphate (DFP), leupeptin, tosyl-L-lysine chloroethyl ketone (TLCK), dimethylformamide (DMF), Luminol (5-amino-2,3-dihydro-1,4-phthalazinedione), Phorbol 12-myristate 13-acetate (PMA), horse-radish peroxidase (HRPO), cytochrome *c* (from horse heart, type VI), latex beads (3 µM), heparin-agarose and L-α-phosphatidylcholine type II-S were obtained from Sigma Chemical Co. (St Louis, MO, USA). Taq DNA polymerase, ATP, guanosine 5'-3-*O*- (thio) triphosphate (GTPγS), NADPH, pepstatin, phenylmethyl sulfonyl fluoride (PMSF) and N-octyl glucoside were from Roche (Meylan, France). Endofree Plasmid Maxi Kit was purchased from QIAGEN (Courtaboeuf, France). The Sephaglas kit and molecular weight markers were from Amersham (Buckinghamshire UK). ECL Western blotting detection reagents, CM Sepharose CL-6B, DEAE Sepharose CL-6B, octyl Sepharose CL-4B and Sephacryl S-300 HR were from Amersham Biosciences, Biotechnology (Uppsala, Sweden). Geneticin (G418) was purchased from Gibco (Cergy Pontoise, France). Monoclonal antibodies mAb449 and mAb48 were kindly provided by Dr. D. Roos (CLB, Amsterdam, the Netherlands). Polyclonal antibody anti-$p47^{phox}$ was purchased from Upstate Biotechnology, Inc. (New York, NY, USA). Monoclonal antibody anti-$gp91^{phox}$, 7D5 was purchased from MBL Medical & Biological Laboratories Co., Ltd. (NaKa-ku Nagoya, Japan). Fetal bovine serum and RPMI 1640 were from Life Technologies, Inc. (Paisley, Scotland, UK). The cDNA encoding $p47^{phox}$ cloned into the plasmid pGEX-2T was kindly provided by A.W. Segal and F. Wientjes (Department of Medicine, University College London, London, UK).

Culture and differentiation of PLB-985 cells

WT, X-CGD and transfected PLB-985 cells expressing WT or the mutant Nox2 were grown in RPMI-1640 medium supplemented with 2 mM glutamine, 10% (v/v) fetal bovine serum, penicillin (100 U/ml), streptomycin (100 µg/ml) in a humidified incubator at 37°C in an atmosphere of 5% CO_2 in air. After selection, 0.5 mg/ml G418 was added to maintain the selection pressure. For granulocytic differentiation, WT or derivative PLB-985 cells (5×10^5 cells/ml) were exposed to 0.5% DMF for 5–7 days [19, 21].

Construction of transfected PLB-985 cell line

Leu505Arg mutation was generated by the replacement of thymine1526 with guanine in the wild-type (WT) Nox2 cDNA in pBluescript II KS (+) vector using the QuikChange site-directed mutagenesis kit

(Stratagene) according to the manufacturer's instructions and subcloned into the mammalian expression vector pEF-PGKneo [19, 21]. The Leu505Arg Nox2 expression construct was sequenced to confirm the mutation and was electroporated into X-CGD PLB-985 cells. Following electroporation, clones were selected by limiting the dilution in 1.5 mg/ml G418.

Cytosol and membrane fraction preparation

After being treated with 3 mM DFP for 15 min on ice, PLB-985 cells or human neutrophils were resuspended at a concentration of 5×10^8 cells/ml in PBS containing 1 mM PMSF, 2 µM leupeptin, 2 µM pepstatin and 10 µM TLCK. Cells were disrupted by sonication 3 × 10 s at 40 W using a Branson sonifier. The homogenate was centrifuged at 1,000 *g* for 15 min at 4°C to remove unbroken cells and nuclei. The postnuclear supernatant was centrifuged at 200,000 *g* for 1 h at 4°C. This high-speed supernatant was referred to as the cytosol and the pellet consisting of crude membranes was suspended in the same buffer [22-27].

Purification and relipidation of cytochrome b_{558} from transfected PLB-985 cells

Cytochrome b_{558} was purified [24]. Briefly, crude membrane pellets from 1.5×10^{10} WT or mutant Nox2-transfected PLB-985 cells were treated with 1 M NaCl to eliminate the contamination of myeloperoxidase and solubilized in 2% N-octyl glucoside (w/v). After a centrifugation at 200,000 *g* for 60 min at 4°C, the supernatant was submitted to three successive chromatographic steps [24, 25]. Purified cytochrome b_{558} was relipidated with L-α-phosphatidylcholine II-S [25-26]. Cytochrome b_{558} purity was assessed by silver-stained SDS-PAGE and Western blotting. Cytochrome b_{558} was quantified by reduced-minus-oxidized difference spectroscopy using Soret band absorption at 426 nm. Liposomes were stored at –80°C.

Purification of recombinant $p67^{phox}$, $p47^{phox}$, and Rac1

Full-length cDNAs encoding $p67^{phox}$, $p47^{phox}$, and Rac1 were expressed in *Escherichia coli* as a glutathione S-transferase fusion protein using pGEX-3X ($p67^{phox}$) or pGEX-2T ($p47^{phox}$ and Rac1). Fusion proteins were purified by affinity glutathione-Sepharose and were incubated with Xa factor for $p67^{phox}$ or thrombin for $p47^{phox}$. Rac1 was cleaved directly on the affinity column [26-27]. Recombinant proteins were stored at –20°C.

FACS analysis, Western blotting and spectral assessment of Nox2 expression in PLB-985 cells

Nox2 expression in intact PLB-985 cells was assessed by using mAb 7D5 (5 µg/ml) [28] or control monoclonal IgG1 (Immunotech, Marseille, France). The expression of cytochrome b_{558} was examined by Western blot using mAb 48 and mAb 449 directed against Nox2 and $p22^{phox}$, respectively [19, 21].

The WT or mutant Nox2 expression was further detected indirectly by cytochrome b_{558} differential spectral analysis. A molecular absorption coefficient of Σ426 nm=106 $mM^{-1}\times cm^{-1}$ for the Soret band was used for calculations [29]. All experiments were done in triplicate.

NADPH oxidase activity in intact cells

H_2O_2 production was measured by chemiluminescence [19, 21]. Granulocyte-differentiated PLB-985 cells (5×10^5 cells/well in a 96-well plate) in PBS containing 0.9 mM Ca^{2+}, 0.5 mM Mg^{2+}, 20 mM glucose, 20 µM luminol and 10 U/ml HRPO were stimulated with PMA (80 ng/ml). Relative light units (RLU) were recorded at 37°C over a time course of 60 min in a luminoscan luminometer (Labsystem, Helsinki, Finland), connected to a computer.

NADPH oxidase and iodonitrotetrazolium (INT) reductase activities in a cell-free-system (CFS) assay

In vitro NADPH oxidase activity was measured using plasma membranes (30 µg) obtained from transfected PLB-985 cells and cytosol (300 µg) from human neutrophils in a reaction mixture containing 20 mM Glucose, 20 µM GTPγS, 5 mM $MgCl_2$, and an optimal amount of arachidonic acid in a final volume of 100 µl [30]. INT reductase activity was performed as described above except that cytochrome *c* was replaced by INT whose reduction was SOD-insensitive [19]. In some experiments, plasma membranes of PLB-985 cells and cytosol of neutrophils were replaced by purified cytochrome b_{558} (0.2 pmol) and purified recombinant proteins, 300 nM $p67^{phox}$, 323 nM $p47^{phox}$ and 100 nM Rac1. We added 10 µM FAD to the reaction medium when purified cytochrome b_{558} was used.

$P47^{phox}$ translocation in transfected PLB-985 cells

$P47^{phox}$ translocation in transfected PLB-985 cells was detected by confocal microscopy analysis. The polyclonal anti-$p47^{phox}$ antibody and mAb 7D5 were used as primary antibodies, Alexa Fluor® 488 $F(ab')_2$ goat anti-rabbit IgG (H+L) and Alexa Fluor® 546 $F(ab')_2$ goat anti-mouse IgG (H+L) (Molecular Probes, Eugene, OR, USA) were added to the system as secondary antibodies. Nuclei were visualized by TO-PRO 3 iodide. Cells were examined with a confocal laser scanning microscope and analyzed with Leica confocal software (Heidelberg, Germany) [19].

***In vitro* translocation of cytosolic NADPH oxidase proteins**

The translocation of $p67^{phox}$, $p47^{phox}$ and Rac to the plasma membrane was studied using a classical method [19, 21]. Briefly, partially purified PLB-985 cell membranes (100 µg) and human neutrophil cytosol (1000 µg) were stimulated with or without 100 µM SDS and 20 µM GTPγS. The re-isolated membrane fraction from a discontinuous sucrose gradient was analyzed by immunoblot with

anti-peptide polyclonal antibodies directed against p67^{phox}, p47^{phox} and Rac, respectively [26, 31]. Polypeptides corresponding to the C-terminal regions of p47^{phox} (residues 371–390) and of p67^{phox} (residues 511–526), and to a peptide (residues 123–145) of Rac1 or Rac2, were synthesized by Neosystem (Strasbourg, France) [31].

Kinetic analysis

Kinetic parameters of NADPH oxidase were determined by a nonlinear regression fit of the data to the Michaelis-Menten equation.

Protein determination

Protein content was estimated using the Bradford assay [32] or the Pierce^{R} method [33].

The three-dimensional (3D) model of the cytosolic part of gp91^{phox}

With the program PyMol, a picture of the 3D model from the C-terminal domain of gp91^{phox} was made and the C-terminal α-helix (residues 483–507) was highlighted [13].

RESULTS AND DISCUSSION

A rare X-linked CGD variant resulting from a missense mutation Leu505Arg has recently been reported [20]. This mutant was characterized by a normal level of a nonfunctional cytochrome b_{558} in the patient's neutrophils, with a totally abolished NADPH oxidase activity. Homologous sequence analysis showed that Leu^{505} is highly conserved in the human Nox-Duox family, except in Nox2 of *Dictyostelium discoideum* and plants in which Leu^{505} is replaced by Phe and Thr (Figure 1A). The conserved characterization of Leu^{505} suggests that this amino acid residue has a common function. According to the sequence alignment of the ferredoxin-$NADP^+$ reductase family (FNR), Leu^{505} is located in the potential adenine-binding motif of NADPH of Nox2. Interestingly, the Nox-Duox family possesses an additional sequence (residues 484–504) just above this amino acid compared to most FNR members (Figure 1B). This region has an α-helical loop structure predicted by the 3D model of the Nox2 C-terminal tail. It has been proposed that it is involved in the binding of cytosolic factors during the time course of oxidase activation, promoting the NADPH access to its binding site [13]. To investigate the molecular mechanism by which the Leu505Arg mutant inhibits the NADPH oxidase activity, a cellular model of this X^+-CGD case was built in the X-CGD PLB-985 cell line previously used to study other $X91^+$-CGD mutations [19, 21].

Leu505Arg Nox2 transfected X-CGD PLB-985 cells mimic $X91^+$-CGD neutrophils

As shown in Figure 2A, FACS analysis showed that the expression level of WT and mutant Nox2 in transfected X-CGD PLB-985 cells was similar to that of the original WT PLB-985 cells [28]. A similar amount of cytochrome b_{558} was observed by immunoblotting (Figure 2B). In addition, the reduced-minus-oxidized difference spectrum of transfected PLB-985 cells was similar to that of WT PLB-985 cells (Figure 2C and Table1), suggesting that the mutant cytochrome b_{558} was correctly processed and targeted to the plasma membrane with heme incorporation. While no Nox2 and cytochrome b_{558} was detected in X-CGD PLB-985 cells or empty vector transfected cells (Figure 2), consistent with the hypothesis that the two subunits of cytochrome b_{558} can co-stabilize each other in the granulocytic cell line [19, 21]. The NADPH oxidase activity of the Leu505Arg Nox2 transfected PLB-985 cells was determined in intact cells. After DMF-induced granulocytic differentiation, H_2O_2 production was measured by luminol-amplified chemiluminescence after activation with 80 ng/ml PMA. WT Nox2 transfected PLB-985 cells had an H_2O_2 production comparable to the original WT PLB-985 cells, as illustrated in Table 1. Even though the expression of Leu505Arg Nox2 was normal,

this mutant was unable to generate H_2O_2, as observed in X-CGD PLB-985 cells or empty vector transfected cells (Table 1). In conclusion, Leu505Arg Nox2 transfected PLB-985 cells mimic the phenotype of $X91^+$-CGD neutrophils [20]. Transfected X-CGD PLB-985 cells had been previously used to study successfully the impact of three Nox2 mutations (Δ488–497, His303Gln/Pro304Arg and Asp500Gly), resulting in $X91^+$-CGD on the NADPH oxidase activation [19, 21, 34]. This confirms that the X-CGD PLB-985 cell line is a useful cellular model to express recombinant Nox2 mutant forms for its structure-function analysis [19, 21, 34].

NADPH oxidase and INT reductase activities in a CFS

Roughly 50% of the NADPH oxidase activity reconstituted with in membranes from WT PLB-985 cells was obtained with membranes from Leu505Arg Nox2 mutant cells. Similarly, INT reductase activity was half of the activity measured in WT PLB-985 cell membranes (Figure 3). In a previous study investigating several Nox2 mutants with the same approach, we found that for most of the mutants, results obtained *in vitro* were correlated with those obtained in intact cells, although residual oxidase activity (20% of the original WT PLB-985 cells) was observed in some mutants that had no oxidase activity *in vivo* [19]. Arachidonic acid probably leads to a conformational change in cytosolic proteins, promoting higher protein–protein interactions than occurs *in vivo*. This suggests that in a CFS assay, the oxidase complex of the Leu505Arg Nox2 assembled and the electron transfer from NADPH to molecular oxygen occurs but under optimal efficiency.

Translocation of cytosolic components of the NADPH oxidase complex

Because Leu^{505} is located near the C-terminal α-helical loop, a potential binding site for $p47^{phox}$ and/or $p67^{phox}$ in Nox2, $p47^{phox}$ translocation was studied in intact transfected PLB-985 cells [19]. As shown in Figure 4A, red and green fluorescence, representing Nox2 and $p47^{phox}$, respectively, surrounded phagosomal membranes around latex beads in both Leu505Arg and WT Nox2 transfected cells. However, it seems that the yellow merged image of the $p47^{phox}$ and Nox2 co-localization was more intense in WT Nox2 transfected PLB-985 cells than in Nox2 mutant cells. Two series of experiments were done with the same result. No $p47^{phox}$ translocation occurred in the X-CGD PLB-985 cells (data not shown) or empty vector transfected cells, demonstrating that this translocation is cytochrome b_{558}-dependent. Similar results were obtained from *in vitro* oxidase cytosolic component translocation experiments. Translocation of $p47^{phox}$ or $p67^{phox}$ to the plasma membrane is visible in both mutant and WT Nox2 transfected cells (Figure 4B), while the efficiency of $p67^{phox}$ translocation seems to be lower in mutated than in WT plasma membrane. These results suggest that in Leu505Arg Nox2 cells, $p47^{phox}$

and p67^{phox} translocation occurred but probably with a lower level of efficiency than in WT Nox2 PLB-985 cells, especially for the p67^{phox} translocation. This can explain the diminished oxidase activity in the *in vitro* reconstituted CFS from Leu505Arg Nox2 mutant membranes. However, in some X91^{+}-CGD cases, cytosolic factor translocation can occur normally even if oxidase activity is abolished [34, 35]. As shown in Figure 4B, Rac translocation is normal in plasma membranes from empty vector transfected X-CGD PLB-985 cells, suggesting that its translocation is independent of the presence of cytochrome b_{558}, as has been observed before [5].

Turnover and K_m for NADPH of WT and Leu505Arg mutant cytochrome b_{558}

According to the sequence alignment study in the FNR reductase family, Leu^{505} is potentially located in the adenine of NADPH-binding site of Nox2 (Figure 1A) [2, 12]. It was of interest to investigate the affinity of the purified mutant flavocytochrome b_{558} for NADPH. Cytochrome b_{558} was purified to homogeneity from 1.5×10^{10} intact WT or mutant Nox2 transfected PLB-985 cells after three successive chromatographic steps. Crude membranes from WT or mutant Nox2-transfected PLB-985 cells contain about 70 pmol of cytochrome b_{558}/mg of proteins, seven times less than what is found in human neutrophils (460 pmol/ mg). This result is consistent with the amount of cytochrome b_{558} found in soluble extract from WT or Leu505Arg transfected PLB-985 cells of 25 pmol/mg versus 170 pmol/mg in human neutrophils [20]. These results suggest that the level of membrane-bound cytochrome b_{558} in PLB-985 cells is about seven times less than in neutrophils. The purified preparation was enriched in cytochrome b_{558} (2800–3500 pmol/mg protein) with a purification factor of 47–50 and a yield of 4–7% (Figure 5C). In the purified proteins, two major bands corresponding to the large and small subunits of cytochrome b_{558}, were observed using immunoblot analysis (Figure 5A). Reduced minus oxidized difference spectra of purified cytochrome b_{558} from both mutant and WT transfected PLB-985 cells possess the three characteristic peaks at 426 nm, 530 and 558 nm (Figure 5B).

The K_m for NADPH and NADH was determined using purified cytochrome b_{558} in presence of neutrophil cytosol or recombinant proteins p67^{phox}, p47^{phox} and Rac1, as detailed in "Experimental Procedure". The K_m of purified WT and Leu505Arg mutant cytochrome b_{558} for NADPH and NADH was determined using increasing NADPH concentrations with optimal conditions in a CFS assay. As shown in Figure 6, the K_m for NADPH of WT cytochrome b_{558} in a CFS assay using neutrophil cytosol and recombinant proteins was 42.2 µM and 46.7 µM, respectively (Figure 6A and 6B, Table 2). Like several FNR reductases, the phagocytic oxidase can utilize NADH as substrate but with a lower affinity

than for NADPH [36]. Indeed the K_m for NADH of purified WT cytochrome b_{558} was 490.1 µM. Our K_m values for NADPH and NADH are in agreement with those obtained by several groups [26, 37-38]. However, the K_m for NADPH and NADH of the purified mutant cytochrome b_{558} was approximately threefold higher than those of the purified WT cytochrome b_{558} (Figure 6A and 6B, Table 2). These data suggest that Leu505Arg mutation disturbed the affinity of the mutant cytochrome b_{558} for NADPH and NADH, while we cannot conclude that this amino acid is directly involved on the binding of these nucleotides. Generally, mutations of an amino acid directly involved in the substrate binding has a dramatic effect on its K_m. This is also true of the Pro415His mutation found in an X91$^+$-CGD patient [39]. The binding of the photoaffinity ligand 2-azido-NADP$^+$ was decreased in the neutrophil membrane from the patient [11]. According to Taylor's model of the C-terminal tail of Nox2, Pro^{415} is the equivalent of Pro^{176} in FNR, lying in the cleft between the NADP and flavin-binding domains to approach the flavin ring involved in electron transfer [10-12]. In our case, there is an electron transfer between NADPH and FAD in the mutant cytochrome b_{558} according to the INT and cytochrome *c* reduction assay (Figure 3).

The turnover of the WT and mutant Leu505Arg purified cytochrome b_{558} in a CFS assay was measured with optimal conditions, as previously described [27, 31]. The oxidase turnover of the purified mutant Leu505Arg cytochrome b_{558} was 112 ± 8 and 63 ± 7 mol $O_2^-.s^{-1}$. mol^{-1} heme *b* when cytosol or recombinant proteins p67^{phox}, p47^{phox} and Rac1 were used, respectively (Figure 6A and 6B). This represents a loss of 35–45% of the oxidase turnover of WT cytochrome b_{558} in a reconstituted CFS using human neutrophil cytosol or recombinant cytosolic factors. This suggests that 1) Part of the NADPH oxidase activity of the purified mutant Leu505Arg cytochrome b_{558} can be restored using neutrophil cytosol or recombinant proteins p67^{phox}, p47^{phox} and Rac1; and 2) The Leu505Arg mutation affects the cytochrome b_{558}, leading to a decrease in maximal specific oxidase activity. We can note that the oxidase turnover was higher when human neutrophil cytosol was used instead of purified recombinant cytosolic factors. Perhaps new partners of oxidase-like MRP8/MRP14 (myeloid-related proteins) present in cytosol improved the NADPH oxidase activity [22].

Effect of increasing the amount of recombinant p67^{phox} on purified Leu505Arg cytochrome b_{558}

According to the slight but reproducible defect of p67^{phox} translocation to the plasma membrane from the mutant transfected PLB-985 cells, the effect of increasing the amount of recombinant p67^{phox} was evaluated on NADPH oxidase activity in a simplified CFS assay using an optimal concentration of purified WT and Leu505Arg mutant cytochrome b_{558}, recombinant proteins Rac1 and p47^{phox} in the

presence of NADPH. As shown in Figure 7, a concentration of 900 nM $p67^{phox}$ was needed to reach optimal NADPH oxidase activity for the Leu505Arg mutant, while only a concentration of 300 nM was sufficient for the WT flavocytochrome b_{558}. In addition, the maximal turnover of NADPH oxidase was 120 mol O_2^-.s^{-1}. mol^{-1} heme *b* for the WT cytochrome b_{558}, while this turnover was 90 mol O_2^-.s^{-1}. mol^{-1} heme *b* for the mutant. It was concluded that the binding efficiency of $p67^{phox}$ on the mutant cytochrome b_{558} was diminished by the Leu505Arg mutation. It appears that more $p67^{phox}$ protein is needed to obtain an active conformation of mutant Nox2 and of the flavocytochrome b_{558}.

Structural context of the Leu^{505} in $gp91^{phox}$

According to the sequence alignment of cytochrome b_{558} with members of the FNR family, it was generally admitted that the ^{504}GLKQ^{507} sequence was a potential site for the adenine-binding site of NADPH [5, 12, 13, 40]. However, Taylor *et al.* (1993) emphasized that despite a high similitude of sequences between the FNR family and the flavocytochrome b_{558}, the most remarkable difference was the addition of a large insertion of 20 residues 484–504, forming an α-helical loop lying directly over the nucleotide-binding cleft. According to the 3D model of the C-terminal tail of Nox2, which was built from the atomic structure of ferredoxin-$NADP^+$ reductase [41], the location of the large insert impaired accessibility to the nucleotide-binding site from the cytosol (Figure 8A and 8B).

This structural element (484–504) contains a highly charged sequence ^{494}HHDEEKD^{500}. In addition to Leu505Arg, two other mutations leading to $X91^+$-CGD have been mapped in this region. They correspond to the deletion of the lower part of the helical insertion, Δ488–497, and to an amino acid substitution, Asp500Gly, in its middle (Figure 8C) [18, 34]. Moreover, we have recently reported that other mutations (notably Asp484Thr, His490Thr and Asp500Gly/Ala/Arg) impair the electron transfer process from NADPH to FAD [19] (Figure 8C). For all the mutants reported in this inserted sequence (associated or not to a known $X91^+$-CGD), the expression level of membrane cytochrome b_{558} as well as the heme difference spectra were comparable to that of WT $gp91^{phox}$ [18, 19, 34]. This indicates that this insertion is not of structural importance for $gp91^{phox}$ integrity. The defective electron transfer from NADPH to FAD in Asp500Gly/Ala/Arg mutants may result from the disrupted interaction between the cytosolic factors with these mutants. Interestingly, Leusen *et al.* [17] found that Asp^{500} was involved in the binding of cytosolic components. A synthetic peptide mimicking domains 491–504 of Nox2 inhibited NADPH oxidase activity in the CFS assay. These data provided evidence that these residues are indispensable for NADPH oxidase assembly related to electron transfer. Monoclonal antibody NL7, which binds the ^{498}EKDVITGLK^{506} region of $gp91^{phox}$, inhibits the NADPH

oxidase activity before or during the initial stages of electron transfer [42]. These data suggest that residues 498–506 of gp91^{phox} participate in the oxidase activation and influence electron transport during superoxide generation.

On the basis of the 3D model analysis, Leu^{505} is at the end of this strategic helix in the C-terminal of gp91^{phox} that may control the entry of NADPH into the cleft of the NADPH-binding site (Figure 8C). Leu^{505} seems not to be directly involved in the binding of the adenine moiety of NADPH but rather a residue located on the protein surface and probably important for some molecular interactions in the activated complex. The conformational change caused by the Leu505Arg may disturb the final oxidase complex assembly. The observation that this Leu505Arg mutant needs larger amounts of p67^{phox} to reach its maximal turnover suggests a possible role in p67^{phox} interaction during activation. In p67^{phox}, region 199–210 was defined from functional studies of various truncated forms of p67^{phox} as an NADPH oxidase activation domain [43]. This domain has been extended, on the basis of structural studies, to the amino acids 187–210 [44] and was reported to be involved in the regulation of the electron transfer [45]. On the gp91^{phox} counterpart, to activate the electron flow, it has been suggested that the movement of the α-helical insertion would be necessary for NADPH entry. A direct link of a conformational change during the oxidase assembly, such as a consequence of an interaction with p67^{phox}, and more precisely its activation domain, can be hypothesized. The Leu505Arg mutant properties are in agreement with such an activation scheme.

FOOTNOTES

Supported by grants from the Université Joseph Fourier, Faculté de Médecine; the Région Rhône-Alpes, programme Emergence; the Ministère de l'Education et de la Recherche; MENRT; and the Direction de la Recherche Régionale Clinique, DRRC. Laboratoire Merck-Sharp and Dohme-Chibret, Programme conjoint de recherche Tempra/Mira 2001-Région Rhône-Alpes

The authors are grateful to Dr. Mary C. Dinauer for the generous gift of WT PLB-985 cells and X-CGD PLB-985 cells. The authors are also grateful to Dr. W. Taylor for the coordinate of the structural model of the C-terminal domain of flavocytochrome b_{558}. The antibodies 449 and 48 were generous gifts from Dr. D. Roos. We thank Pr. Philippe Gaudin for financial support and Michelle Guillot for technical assistance.

Abbreviations used: CGD, chronic granulomatous disease; PMA, Phorbol 12-myristate 13-acetate; fMLP, formyl-methionylleucyl-phenylalanine; DMF, dimethylformamide; SOD, superoxide dismutase; DFP, diisopropylfluorophosphate; PMSF, phenylmethyl sulfonyl fluoride; mAb, monoclonal antibody; FNR, ferredoxin-$NADP^+$ reductase; cyt *b*, cytochrome b_{558}; RP, recombinant protein; Mem, membrane.

REFERENCES

1. Babior, B. M. (2004) NADPH oxidase. Curr. Opin. Immunol. 16, 42-47
2. Vignais, P. V. (2002) The superoxide-generating NADPH oxidase: structural aspects and activation mechanism. Cell. Mol. Life Sci. 59, 1428-1459
3. Lapouge, K., Smith, S. J., Groemping, Y., Rittinger, K. (2002) Architecture of the p40-p47-p67phox complex in the resting state of the NADPH oxidase. A central role for p67phox. J. Biol. Chem. 277, 10121–10128
4. Groemping, Y., Rittinger K. (2005) Activation and assembly of the NADPH oxidase: a structural perspective. Biochem. J. 386, 401-416
5. Heyworth, P. G., Bohl, B. P., Bokoch, G. M., Curnutte, J. T. (1994) Rac translocates independently of the neutrophil NADPH oxidase components p47phox and p67phox. Evidence for its interaction with flavocytochrome b_{558}. J. Biol. Chem. 269, 30749-30752
6. Cross, A. R., Rae, J., Curnutte, J. T. (1995) Cytochrome b_{-245} of the neutrophil superoxide-generating system contains two nonidentical hemes. Potentiometric studies of a mutant form of gp91phox. J. Biol. Chem. 270, 17075-17077
7. Goldblatt, D., Thrasher, A. J. (2000) Chronic granulomatous disease. Clin. Exp. Immunol. 122, 1-9
8. Biberstine-Kinkade, K. J., DeLeo, F. R., Epstein, R. I., LeRoy, B. A., Nauseef , W. M., Dinauer, M. C. (2001) Heme-ligating histidines in flavocytochrome b_{558}: identification of specific histidines in gp91-phox. J. Biol. Chem. 276, 31105-31112
9. Wallach, T. M., Segal, A. W. (1997) Analysis of glycosylation sites on gp91phox, the flavocytochrome of the NADPH oxidase, by site-directed mutagenesis and translation in vitro. Biochem. J. 321, 583-585
10. Sumimoto, H., Sakamoto, N., Nozaki, M., Sakaki, Y., Takeshige, K., Minakami, S. (1992) Cytochrome b_{558}, a component of the phagocyte NADPH oxidase, is a flavoprotein. Biochem. Biophys. Res. Commun. 186, 1368-1375
11. Segal, A. W., West , I., Wientjes, F., Nugent, J. H., Chavan, A. J., Haley, B., Garcia, R. C., Rosen, H., Scrace, G. (1992) Cytochrome b_{-245} is a flavocytochrome containing FAD and the NADPH-binding site of the microbicidal oxidase of phagocytes. Biochem. J. 284, 781-788
12. Rotrosen, D., Yeung, C. L., Leto, T. L., Malech, H. L., Kwong, C. H. (1992) Cytochrome b_{558}: the flavin-binding component of the phagocyte NADPH oxidase. Science 256, 1459-1462

13. Taylor, W. R., Jones, D. T., Segal, A. W. (1993) A structural model for the nucleotide binding domains of the flavocytochrome b_{-245} beta-chain. Protein Sci. 2, 1675-1685
14. Thrasher, A. J., Keep, N. H., Wientjes, F., Segal, A. W. (1994) Chronic granulomatous disease. Biochim. Biophys. Acta. 1227, 1-24.
15. Segal, A. W. (1996) The NADPH oxidase and chronic granulomatous disease. Mol. Med. Today 2, 129-135
16. Heyworth, P. G., Cross, A. R., Curnutte, J. T. (2003) Chronic granulomatous disease. Curr. Opin. Immunol. 15, 578-584
17. Leusen, J. H., de Boer, M., Bolscher, B. G., Hilarius, P. M., Weening, R. S., Ochs, H. D., Roos, D., Verhoeven, A. J. (1994) A point mutation in gp91-phox of cytochrome b_{558} of the human NADPH oxidase leading to defective translocation of the cytosolic proteins p47-phox and p67-phox. J. Clin. Invest. 93, 2120-2126
18. Yoshida, L. S., Saruta, F., Yoshikawa, K., Tatsuzawa, O., Tsunawaki, S. (1998) Mutation at histidine 338 of gp91-phox depletes FAD and affects expression of cytochrome b_{558} of the human NADPH oxidase. J. Biol. Chem. 273, 27879-27886
19. Li, X. J., Grunwald, D., Mathieu, J., Morel, F., Stasia, M. J. (2005) Crucial role of two potential cytosolic regions of Nox2-191TSSTKTIRRS200 and 484DESQANHFAVHHDEEKD500-on NADPH oxidase activation. J. Biol. Chem. 280, 14962-14973
20. Stasia, M. J., Bordigoni, P., Floret, D., Brion, J. P., Bost-Bru, C., Michel, G., Gatel, P., Durant-Vital, D., Voelckel, M. A., Li, X. J., Guillot, M., Maquet, E., Martel, C., Morel, F. (2005) Characterization of six novel mutations in the CYBB gene leading to different sub-types of X-linked chronic granulomatous disease. Hum. Genet. 116, 72-82
21. Bionda, C., Li, X. J., Bruggen, R. V., Eppink, M., Roos, D., Morel, F., Stasia, M. J. (2004) Functional analysis of two-amino acid substitutions in gp91*phox* in a patient with X-linked flavocytochrome b_{558}-positive chronic granulomatous disease by means of transgenic PLB-985 cells. Hum. Genet. 115, 418-427
22. Berthier, S., Paclet, M. H., Lerouge, S., Roux, F., Vergnaud, S., Coleman, A. W., Morel, F. (2003) Changing the conformation state of cytochrome b_{558} initiates NADPH oxidase activation: MRP8/MRP14 regulation. J. Biol. Chem. 278, 25499-25508

23. Parkos, C. A., Allen, R. A., Cochrane, C. G., Jesaitis, A. J. (1987) Purified cytochrome b from human granulocyte plasma membrane is comprised of two polypeptides with relative molecular weights of 91,000 and 22,000. J. Clin. Invest. 80, 732-742

24. Batot, G., Martel, C., Capdeville, N., Wientjes, F., Morel, F. (1995) Characterization of neutrophil NADPH oxidase activity reconstituted in a cell-free assay using specific monoclonal antibodies raised against cytochrome b_{558}. Eur. J. Biochem. 234, 208-215

25. Paclet, M. H., Coleman, A. W., Burritt, J., Morel, F. (2001) NADPH oxidase of Epstein-Barr-virus immortalized B lymphocytes. Effect of cytochrome b_{558} glycosylation. Eur. J. Biochem. 268, 5197-5208

26. Abo, A., Boyhan, A., West, I., Thrasher, A. J., Segal, A. W. (1992) Reconstitution of neutrophil NADPH oxidase activity in the cell-free system by four components: p67-phox, p47-phox, p21rac1, and cytochrome b_{-245}. J. Biol. Chem. 267,16767-16770

27. Paclet, M. H., Coleman, A. W., Vergnaud, S., Morel, F. (2000) P67-phox-mediated NADPH oxidase assembly: imaging of cytochrome b_{558} liposomes by atomic force microscopy. Biochemistry 39, 9302-9310

28. Yamauchi, A., Yu, L., Potgens, A. J., Kuribayashi, F., Nunoi, H., Kanegasaki, S., Roos, D., Malech, H. L., Dinauer, M. C., Nakamura, M. (2001) Location of the epitope for 7D5, a monoclonal antibody raised against human flavocytochrome b_{558}, to the extracellular peptide portion of primate gp91phox. Microbiol. Immunol. 45, 249–257

29. Batot, G., Paclet, M. H., Doussière, J., Vergnaud, S., Martel, C., Vignais, P. V., Morel, F. (1998) Biochemical and immunochemical properties of B lymphocyte cytochrome b_{558}. Biochim. Biophys. Acta. 406, 188-202

30. Cohen-Tanugi, L., Morel, F., Pilloud-Dagher, M. C., Seigneurin, J. M., François, P., Bost, M., Vignais, P. V. (1991) Activation of O_2^--generating oxidase in an heterologous cell-free system derived from Epstein-Barr-virus-transformed human B lymphocytes and bovine neutrophils. Application to the study of defects in cytosolic factors in chronic granulomatous disease. Eur. J. Biochem. 202, 649-655

31. Vergnaud, S., Paclet, M. H., El Benna, J., Pocidalo, M. A., Morel, F. (2000) Complementation of NADPH oxidase in p67-phox-deficient CGD patients p67-phox/p40-phox interaction. Eur. J. Biochem. 267, 1059-1067

32. Bradford, M. M. (1976) A rapid and sensitive method for the quantitation of microgram quantities of protein utilizing the principle of protein-dye binding. Anal. Biochem. 72, 248-254

33. Smith, P. K., Krohn, R. I., Hermanson, G. T., Mallia, A. K., Gartner, F. H., Provenzano, M. D., Fujimoto, E. K., Goeke, N. M., Olson, B. J., Klenk,D. C. (1985) Measurement of protein using bicinchoninic acid. Anal. Biochem. 150, 76-85

34. Yu, L., Cross, A. R., Zhen, L., Dinauer, M. C. (1999) Functional analysis of NADPH oxidase in granulocytic cells expressing a delta488-497 gp91phox deletion mutant. Blood 94, 2497-2504

35. Azuma, H., Oomi, H., Sasaki, K., Kawabata, I., Sakaino, T., Koyano, S., Suzutani, T., Nunoi, H., Okuno, A. (1995) A new mutation in exon 12 of the gp91-phox gene leading to cytochrome b-positive X-linked chronic granulomatous disease. Blood 85, 3274-3277

36. Babior, B. M. (1984) The respiratory burst of phagocytes. J. Clin. Invest. 73, 599-601

37. Koshkin, V., Lotan, O., Pick, E. (1996) The cytosolic component p47phox is not a sine qua non participant in the activation of NADPH oxidase but is required for optimal superoxide production. J. Biol. Chem. 271, 30326-30329

38. Nisimoto, Y., Motalebi S., Han, C. H., Lambeth, J. D. (1999) The p67phox activation domain regulates electron flow from NADPH to flavin in flavocytochrome b_{558}. J. Biol. Chem. 274, 22999-23005

39. Dinauer, M. C., Curnutte, J. T., Rosen, H., Orkin, S. H. (1989) A missense mutation in the neutrophil cytochrome b heavy chain in cytochrome-positive X-linked chronic granulomatous disease. J. Clin. Invest. 84, 2012-2016

40. Suh, Y. A., Arnold, R. S., Lassegue, B., Shi, J., Xu, X., Sorescu, D., Chung, A. B., Griendling, K. K., Lambeth, J. D. (1999) Cell transformation by the superoxide-generating oxidase Mox1. Nature 401, 79-82

41. Karplus, P.A., Daniels, M. J., Herriott, J. R. (1991) Atomic structure of ferredoxin-NADP+ reductase: prototype for a structurally novel flavoenzyme family. Science 251, 60-66

42. Burritt, J. B., Foubert, T. R., Baniulis, D., Lord, C. I., Taylor, R. M., Mills, J. S., Baughan, T. D., Roos, D., Parkos, C. A., Jesaitis, A. J. (2003) Functional epitope on human neutrophil flavocytochrome b_{558}. J. Immunol. 170, 6082-6089

43. Han, C. H., Freeman, J. L., Lee, T., Motalebi, S. A., Lambeth, J. D. (1998) Regulation of the neutrophil respiratory burst oxidase. Identification of an activation domain in p67phox. J. Biol. Chem. 273, 16663-16668

44. Grizot, S., Fieschi, F., Dagher, M. C., Pebay-Peyroula, E. (2001) The active N-terminal region of p67phox: structure at 1.8 Å resolution and biochemical characterizations of the A128V mutant implicated in chronic granulomatous disease. J. Biol. Chem. 276, 21627–21631

45. Nisimoto, Y., Motalebi S., Han, C. H., Lambeth, J. D. (1999) The p67phox activation domain regulates electron flow from NADPH to flavin in flavocytochrome b_{558}. J. Biol. Chem. 274, 22999-23005

FIGURE LEGENDS

Figure 1 Amino acid sequence alignment of the potential NADPH-binding sites of Nox2 in the Nox/Duox and FNR reductase families

(**A**) The amino acid residues involved in adenine binding are shown in the light shaded column. Leucine 505 is shown in the dark shaded column. (**B**) The putative adenine-binding site in the FNR family from the sequence alignment of Taylor *et al.* Helix-α is shown in the shaded column. YSCFRElA = Essential for ferric reductase activity - *Saccharomyces cerevisiae*; NIA_ASPNI = Nitrate reductase (EC 1.6.6.1) - *Aspergillus nidulans*; NIA_NEUCR = Nitrate reductase (NADPH) (EC 1.6.6.3) - *Neurospora crassa*; B26616 = Cytochrome b5 reductase; NIA_SPIOL = Nitrate reductase (EC 1.6.6.1) (NR) - *Spinacia oleracea* (spinach); S15959 = Nitrate reductase (NAD(P)H) (EC 1.6.6.2) - European white birch; MZENAR = NADH:nitrate reductase (AA at 1) (EC 1.6.6.1) - *Zea mays*; DMPP_PSEPU = Hydroxylase P5 protein (EC 1.14.13.7) phenol 2-mono-oxygenase P5 component - *Pseudomonas*; S15303 = Hypothetical protein 7.6-*Salmonella typhimurium*; MEMC_METCA = Methane monooxygenase component C (EC 1.14.13.25) methane hydroxylase - *Methylococcus capsula*; XYLZ_PSEPU = E 1.2-dioxygenase electron transfer component contains ferredoxin and ferredoxin-NAD(+); PSENAPDOXA = DOXA locus PSENAPDOXA - *Pseudomonas purida*; FENR_ANASO = Ferredoxin-NADP reductase (EC 1.18.1.2) (FNR) - *Anabaena* spp.; SYONDHF = F N-terminal domain homologous to CpcD proteins of *Synechococcus* spp.; N_lFNR = Ferredoxin:$NADP^+$ oxidoreductase (ferredoxin reductase) (EC 1.18.1.2) - *Spinacia olerucea* (spinach)

Figure 2 Expression of WT and mutated Nox2 in transfected X-CGD PLB-985 cells

(**A**) Flow cytometry analysis of Nox2 expression. 5×10^5 differentiated WT or transfected X-CGD PLB-985 cells were incubated with the Nox2 mAb 7D5, as described in "Experimental procedures". Mouse IgG1 isotype was used as an irrelevant mAb. (**B**) Immunoblot analysis of the two subunits of cytochrome b_{558} (Nox2/$p22^{phox}$) was performed with 50 µg of 1% Triton X100 soluble extracts from WT or transfected PLB-985 cells, subjected to SDS-PAGE (10% acrylamide gel), blotted onto a nitrocellulose sheet, and detected with mAb 48 and mAb 449. (**C**) Cytochrome b_{558} differential spectra were performed with the same extract as described in (**B**). Results are from one experiment representative of three.

Figure 3 NADPH oxidase and INT reductase activity in a cell-free system assay

Cytochrome *c* and INT reduction were measured using crude membranes (30 µg) isolated from transfected PLB-985 cells in the presence of neutrophil cytosol (300 µg) and activated with GTPγS, $MgCl_2$ and arachidonic acid, as described in "Experimental procedures". The data represent mean ± SD of three separate experiments.

Figure 4 Analysis of the NADPH oxidase assembly in transfected PLB-985 cells

(**A**) Localization of $p47^{phox}$ and Nox2 during activation of transfected PLB-985 cells. A total of 5×10^5 transfected PLB-985 cells were activated with PMA-treated latex-beads for 15 min on day 6 after 0.5% DMF differentiation. Nox2 and $p47^{phox}$ translocation was followed by confocal microscopy analysis, as described in "Experimental procedures". Polyclonal anti-$p47^{phox}$ antibody and mAb 7D5 were used as primary antibodies, Alexa Fluor® 488 $F(ab')_2$ fragments of goat anti-rabbit IgG (H+L) and Alexa Fluor® 546 $F(ab')_2$ fragments of goat anti-mouse IgG(H+L) were used as second antibodies. Empty vector transfected X-CGD PLB-985 cells were used as the negative control. (**B**) *In vitro* the translocation of $p47^{phox}$, $p67^{phox}$ and Rac to the plasma membrane of transfected PLB-985 cells. NADPH oxidase was activated *in vitro* in presence (+) or in absence (–) of SDS and GTPγS, using crude membrane from transfected PLB-985 cells as described in "Experimental procedures". $P47^{phox}$, $p67^{phox}$ and Rac were detected in the plasma membranes by Western blot after discontinuous sucrose gradient purification.

Figure 5 Purification of cytochrome b_{558} from transfected PLB-985 cells

(**A**) Immunodetection of cytochrome b_{558} was performed with the membrane fractions isolated at each purification step, 3 µg proteins were used for Western blotting with mAb 48 and mAb 449. (**B**) Differential spectral analysis of cytochrome b_{558} purified from transfected PLB-985 cells. Reduction was achieved by adding a few grains of sodium dithionite to the sample, and the reduced-minus-oxidized difference spectra were recorded at room temperature with a DU 640 Beckman spectrophotometer. (**C**) Purification table of cytochrome b_{558} from transfected PLB-985 cells.

Figure 6 Effect of Leu505Arg mutation on K_m for NADPH in the cell-free reconstituted system

(**A**) Activation of NADPH oxidase in a CFS assay using purified cytochrome b_{558} (0.2 pmol) from transfected PLB-985 cells and neutrophil cytosol (300 µg) according to NADPH increasing

concentration (0–1000 µM). (**B**) Activation of NADPH oxidase in a CFS assay was performed as in (**A**), except that neutrophil cytosol was replaced by recombinant cytosolic proteins, $p67^{phox}$ (300 nM), $p47^{phox}$ (323 nM), and Rac1 (100 nM). Data are representative of three independent experiments.

Figure 7 Effect of Leu505Arg mutation on the affinity of cytochrome b_{558} for $p67^{phox}$ in the cell-free reconstituted system

Activation of NADPH oxidase in a CFS assay using purified cytochrome b_{558} (0.2 pmol) from transfected PLB-985 cells and recombinant cytosolic proteins, $p47^{phox}$ (323 nM), Rac1 (100 nM) and increasing concentrations of $p67^{phox}$ (0–1500 nM) in the presence of 300 µM NADPH. Data are representative of three independent experiments.

Figure 8 Surface representation of the 3D model of the cytosolic part of $gp91^{phox}$

(**A**) The surface drawn in blue is a top view from the inside of the membrane. FAD and NADPH are represented as sticks using the CPK color code. The surface of the additional α-helix (residues 483–507), closing access to the NADPH binding-site, is sand-colored. (**B**) The surface structure viewed from the cytoplasm after a 90° rotation in the upper direction of the surface structure presented in (**A**). (**C**) Zoom on the α-helix (residues 483–507) orientated as in (**B**). Leu^{505}, Asp^{500}, His^{490} and Asp^{484} are represented as sticks. The figures were drawn with PyMol.

Table 1

Cytochrome b_{558} amount and NADPH activity in WT and transfected X-CGD PLB-985 cells

The Cytochrome b_{558} concentration in 1% Triton-X100 soluble extracts was quantified using Soret band absorption for WT, X-CGD, and transfected PLB-985 cells, considering that cytochrome b_{558} contains two hemes.

H_2O_2 production was measured by luminol-amplified chemiluminescence in differentiated WT and transfected X-CGD PLB-985 cells after PMA activation. RLU represents the sum of relative luminescence units measured in 60 min. Values in this table represent the mean ± SD of triplicate determinations.

Transfected PLB-985 cells	Cytochrome *b* 558 pmol/mg (n=3)	Chemiluminescence	
		H_2O_2 production (RLU)	% of control
WT PLB-985	25.05 ± 3.43	384.04 ± 10.71	100
WT-Nox2	24.19 ± 1.55	368.81 ± 3.37	96
X-CGD PLB-985	0	0.34 ± 0.07	0
Empty vector	0	0.33 ± 0.06	0
Leu505Arg	28.88 ± 0.61	0.10 ± 0.03	0

Table 2

Specific NADPH oxidase activity and K_m for NADPH and NADH of WT and Leu505Arg cytochrome b_{558}

In vitro NADPH oxidase activity was reconstituted using purified cytochrome b_{558} (0.2 pmol) and neutrophil cytosol (300 µg) or purified recombinant proteins (RP), 300 nM $p67^{phox}$, 323 nM $p47^{phox}$ and 100 nM Rac1. We added 10 µM FAD to the reaction medium containing 20 mM glucose, 20 µM GTPγS, 5 mM $MgCl_2$, and an optimal amount of arachidonic acid in a final volume of 100 µl.

Transfected PLB-985 cells	Specific activity (300 µM NADPH)		K_m		
	Turnover (mol O_2^-/sec/mol heme *b*)		NADPH		NADH
	Cyt *b* + Cytosol	Cyt *b* + RP	Cyt *b* + Cytosol	Cyt *b* + RP	Cyt *b* + RP
WT-Nox2	171 ± 3	119 ± 9	42 µM	47 µM	490 µM
Leu505Arg	112 ± 8	63 ± 7	142 µM	147 µM	1284 µM

A

		Pyrophosphate															Ribose							Adenine					Nicotinamide						
Homo sapiens	Nox2 (gp91phox)	405	M	L	V	G	A	G	I	G	V	T	P	F	416	442	Y	W	L	C	R	446	504	G	L	K	Q	507	535	F	L	C	G	P	E	540
	Nox-1	399	V	L	V	G	A	G	I	G	V	T	P	F	410		-	-	-	-	-		498	G	L	K	Q	501	480	F	L	C	G	P	R	485
	Nox-3	403	V	C	V	A	A	G	I	G	V	T	P	F	414	440	Y	W	I	C	R	444	502	G	L	K	Q	505	533	F	F	C	G	P	K	538
	Nox-4	427	L	C	V	A	G	G	I	G	V	T	P	F	438	460	I	W	V	C	R	464	514	A	L	N	S	520	545	F	C	C	G	P	N	550
	Nox-5	385	V	L	I	G	A	G	I	G	I	T	P	F	396	437	I	W	I	N	R	441	508	G	L	Q	T	511	538	F	F	C	G	S	P	543
	Duox 1	1384	V	L	V	G	G	G	I	G	V	T	P	F	1395	1420	I	W	V	T	R	1424	1486	G	L	R	S	1489	1508	F	S	C	G	P	P	1513
	Duox 2	1381	V	L	V	G	G	G	I	G	V	T	P	F	1392	1417	I	W	V	T	R	1421	1483	G	L	R	S	1486	1515	F	S	C	G	P	P	1520
Rattus	gp91-phox	405	M	L	V	G	A	G	I	G	V	T	P	F	416	442	Y	W	L	C	R	446	504	G	L	K	Q	507	535	F	L	C	G	P	E	540
Mus musculus	gp91-phox	405	M	L	V	G	A	G	I	G	V	T	P	F	416	442	Y	W	L	C	R	446	504	G	L	K	Q	507	535	F	L	C	G	P	E	540
Rattus norvegicus	Endothelial type gp91-phox	405	M	L	V	G	A	G	I	G	V	T	P	S	416	442	Y	W	L	C	R	446	504	G	L	K	Q	507	535	F	L	C	G	P	E	540
pig	NADPH oxidase heavy chain subunit	303	M	L	V	G	A	G	I	G	V	T	P	F	314	340	Y	W	L	C	R	344	402	G	L	K	Q	405	433	F	L	C	G	P	E	438
Oryctolagus cuniculus	gp91-phox	405	M	L	V	G	A	G	I	G	V	T	P	F	416	442	Y	W	L	C	R	446	504	G	L	K	Q	507	535	F	L	C	G	P	E	540
Bos taurus	NADPH oxidase heavy chain	405	M	L	V	G	A	G	I	G	V	T	P	F	416	442	Y	W	L	C	R	446	504	G	L	K	Q	507	535	F	L	C	G	P	E	540
Tursiops truncatus	gp91-phox	405	M	L	V	G	A	G	I	G	V	T	P	F	416	442	Y	W	L	C	R	446	503	G	L	K	Q	506	534	F	L	C	G	P	E	539
Dictyostelium discoideum	NADPH oxidase	357	I	L	V	G	A	G	I	G	V	T	P	F	368	395	Y	W	I	C	R	399	453	G	F	T	T	456	484	F	F	C	G	P	K	489
Emericella nidulans	NADPH oxidase	370	V	L	I	G	T	G	I	G	V	T	P	W	381	407	I	W	V	C	K	411	475	E	L	K	S	478	518	Y	F	C	G	P	N	523
Rice	rboh A-rice	390	L	L	V	G	L	G	I	G	A	T	P	F	401	460	Y	W	V	T	R	464	526	G	T	K	V	529	557	F	Y	C	G	A	P	562
Nicotiana tabacum	NADPH oxidase	761	L	L	V	G	L	G	I	G	A	T	P	F	772	832	Y	W	V	T	R	836	898	G	T	R	V	901	929	F	Y	C	G	A	P	934

B

Nox2 (gp91phox)	476	Y	N	I	-	-	Y	L	T	G	W	D	E	S	Q	A	N	H	F	A	V	H	H	D	E	E	K	D	V	I	T	G	L	K	Q	K	T	L	Y	G	R	513
YSCFREIA	593	Y	T	G	-	-	S	S	V	E	D	T	N	S	D	E	S	T	K	G	F	D	D	K	E	E	S	E	I	T	V	E	C	L	N	K	R	P	D	L	K	630
NIA_ASPNI	812	L	K	T	-	-	G	S	E	S	W	-	-	-	-	-	-	-	-	-	-	-	-	-	-	-	-	-	-	-	-	-	T	G	R	R	G	R	I	D	E	828
NIA_NEUCR	919	L	S	R	-	-	P	G	A	E	W	-	-	-	-	-	-	-	-	-	-	-	-	-	-	-	-	-	-	-	-	-	E	G	L	R	G	R	L	D	K	935
B26616	863	V	E	K	-	-	A	E	E	G	W	-	-	-	-	-	-	-	-	-	-	-	-	-	-	-	-	-	-	-	-	-	K	Y	D	T	G	F	I	S	E	879
NIA_SPIOL	212	L	D	R	-	-	A	P	E	A	W	-	-	-	-	-	-	-	-	-	-	-	-	-	-	-	-	-	-	-	-	-	D	Y	G	Q	G	F	V	N	E	228
S15959	834	V	K	E	-	S	K	R	E	G	W	-	-	-	-	-	-	-	-	-	-	-	-	-	-	-	-	-	-	-	-	-	E	Y	S	V	G	Y	I	R	E	851
MZENAR	555	I	D	Q	-	-	V	E	K	G	W	-	-	-	-	-	-	-	-	-	-	-	-	-	-	-	-	-	-	-	-	-	K	Y	S	V	G	F	V	T	E	571
DMPP_PSEPU	259	L	N	Q	A	N	D	D	P	E	W	-	-	-	-	-	-	-	-	-	-	-	-	-	-	-	-	-	-	-	-	-	Q	G	F	K	G	F	V	H	D	277
S15303	259	V	S	G	-	-	D	D	A	E	W	-	-	-	-	-	-	-	-	-	-	-	-	-	-	-	-	-	-	-	-	-	G	G	R	K	G	F	V	H	H	275
MEMC_METCA	280	V	W	H	-	-	P	S	G	D	W	-	-	-	-	-	-	-	-	-	-	-	-	-	-	-	-	-	-	-	-	-	E	G	E	Q	G	S	P	I	D	296
XYLZ_PSEPU	272	V	A	S	-	-	P	D	S	A	Y	-	-	-	-	-	-	-	-	-	-	-	-	-	-	-	-	-	-	-	-	-	-	P	Q	K	G	Y	V	T	Q	287
PSENAPDOXA	262	I	A	M	-	-	G	P	I	N	E	-	-	-	-	-	-	-	-	-	-	-	-	-	-	-	-	-	-	-	-	-	S	Q	R	A	G	L	V	T	D	278
FENR_ANASO	223	I	S	R	-	-	E	Q	K	N	P	-	-	-	-	-	-	-	-	-	-	-	-	-	-	-	-	-	-	-	-	-	Q	G	G	R	M	Y	I	Q	D	239
SYONDHF	321	I	S	R	-	-	E	Q	K	T	A	-	-	-	-	-	-	-	-	-	-	-	-	-	-	-	-	-	-	-	-	-	D	G	G	K	V	Y	V	Q	S	337
N_IFNR	332	V	S	R	-	-	E	Q	T	N	E	-	-	-	-	-	-	-	-	-	-	-	-	-	-	-	-	-	-	-	-	-	K	G	E	K	M	Y	I	Q	T	348

Figure 1

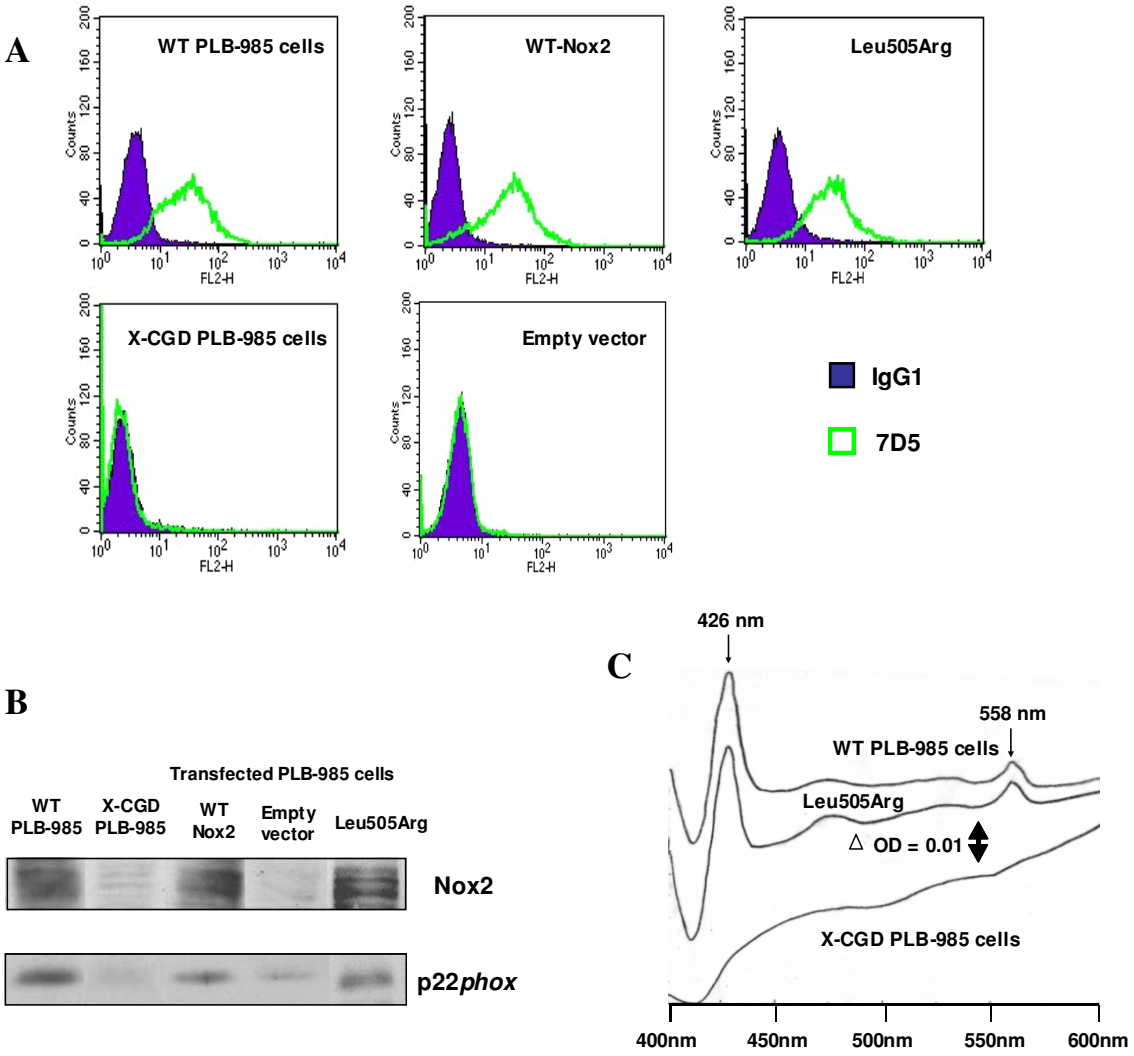
A
WT PLB-985 cells
WT-Nox2
Leu505Arg
X-CGD PLB-985 cells
Empty vector
IgG1
7D5
Counts
FL2-H
B
Transfected PLB-985 cells
WT PLB-985
X-CGD PLB-985
WT Nox2
Empty vector
Leu505Arg
Nox2
p22phox
C
426 nm
558 nm
WT PLB-985 cells
Leu505Arg
△ OD = 0.01
X-CGD PLB-985 cells
400nm
450nm
500nm
550nm
600nm

Figure 2

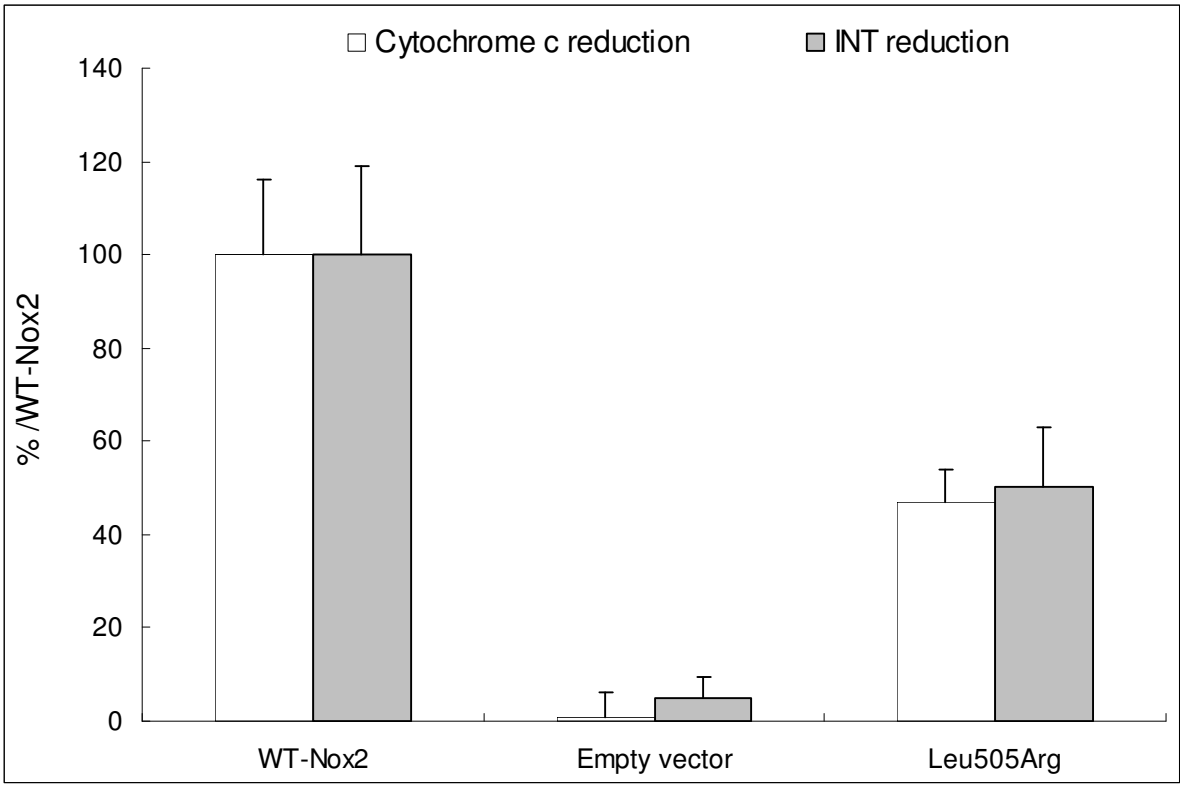
Cytochrome c reduction
INT reduction
140
120
100
80
60
40
20
0
% /WT-Nox2
WT-Nox2
Empty vector
Leu505Arg

Figure 3

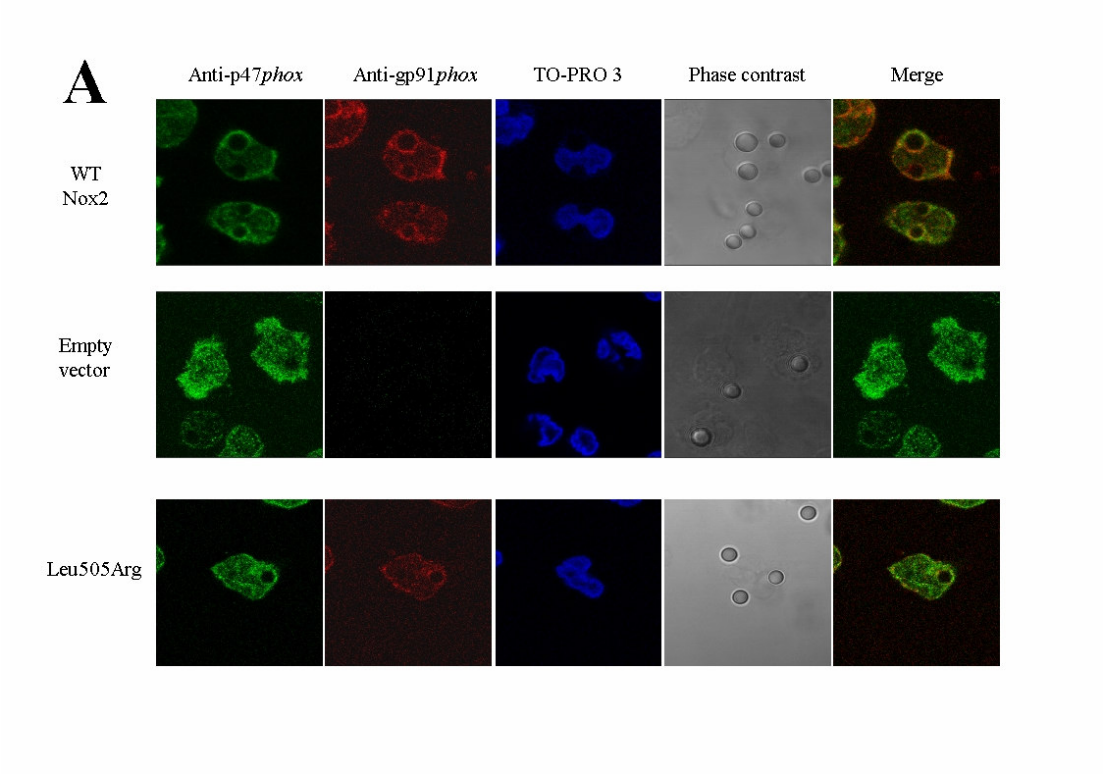
A
Anti-p47*phox*
Anti-gp91*phox*
TO-PRO 3
Phase contrast
Merge
WT Nox2
Empty vector
Leu505Arg
B
WT-Nox2
Empty vector
Leu505Arg
p67*phox*
p47*phox*
Rac
−
+
−
+
−
+

Figure 4

A

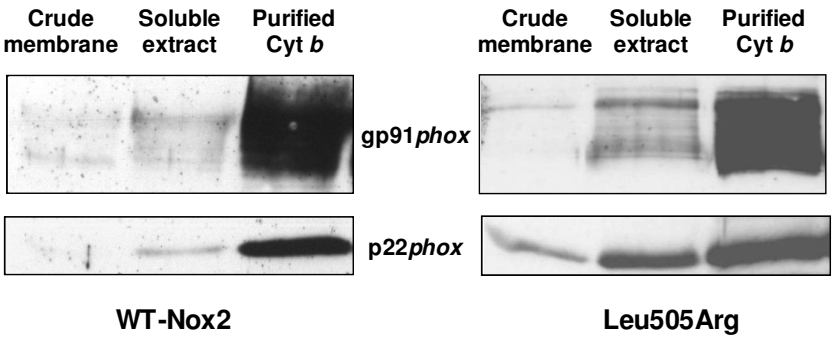

B

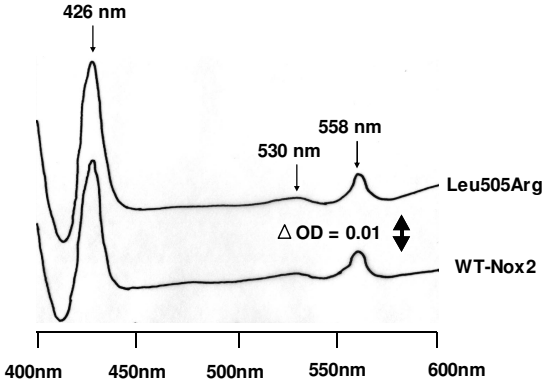

C

Transfected PLB-985 cells	Cyt *b* concentration (pmol/mg)		Cyt *b* purification	
	Crude Mem	Purified Cyt *b*	Purification factor	Yield (%)
WT-Nox2	60	2840	47	7
Leu505Arg	71	3536	50	4

Figure 5

A

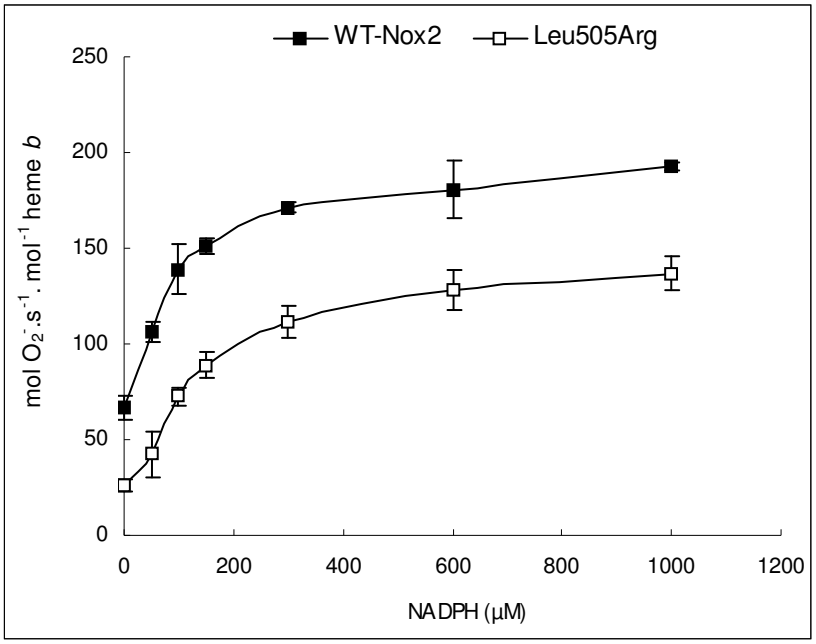
WT-Nox2
Leu505Arg
mol O_2^-.s^{-1}.mol^{-1} heme *b*
250
200
150
100
50
0
0
200
400
600
800
1000
1200
NADPH (µM)

B

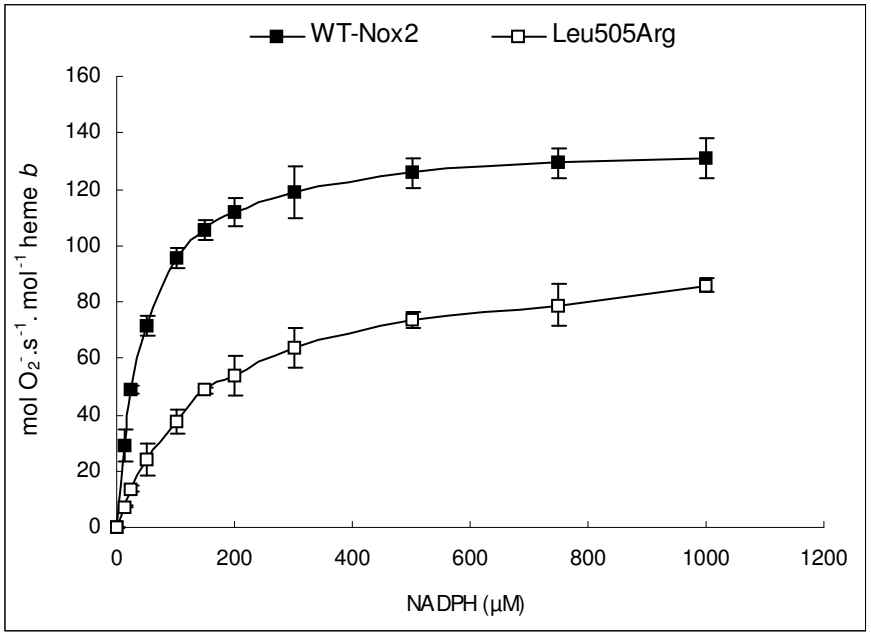
WT-Nox2
Leu505Arg
mol O_2^-.s^{-1}.mol^{-1} heme *b*
160
140
120
100
80
60
40
20
0
0
200
400
600
800
1000
1200
NADPH (µM)

Figure 6

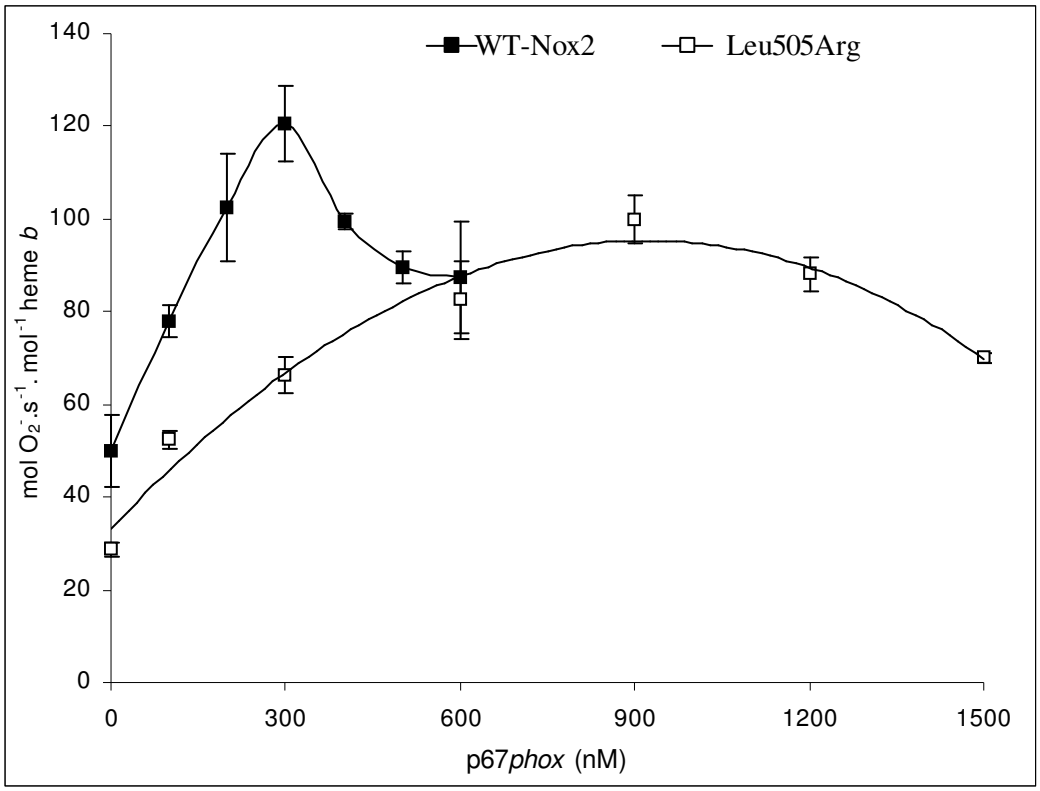
WT-Nox2
Leu505Arg
mol $O_2^{\cdot-}.s^{-1}$. mol^{-1} heme *b*
140
120
100
80
60
40
20
0
0
300
600
900
1200
1500
p67*phox* (nM)

Figure 7

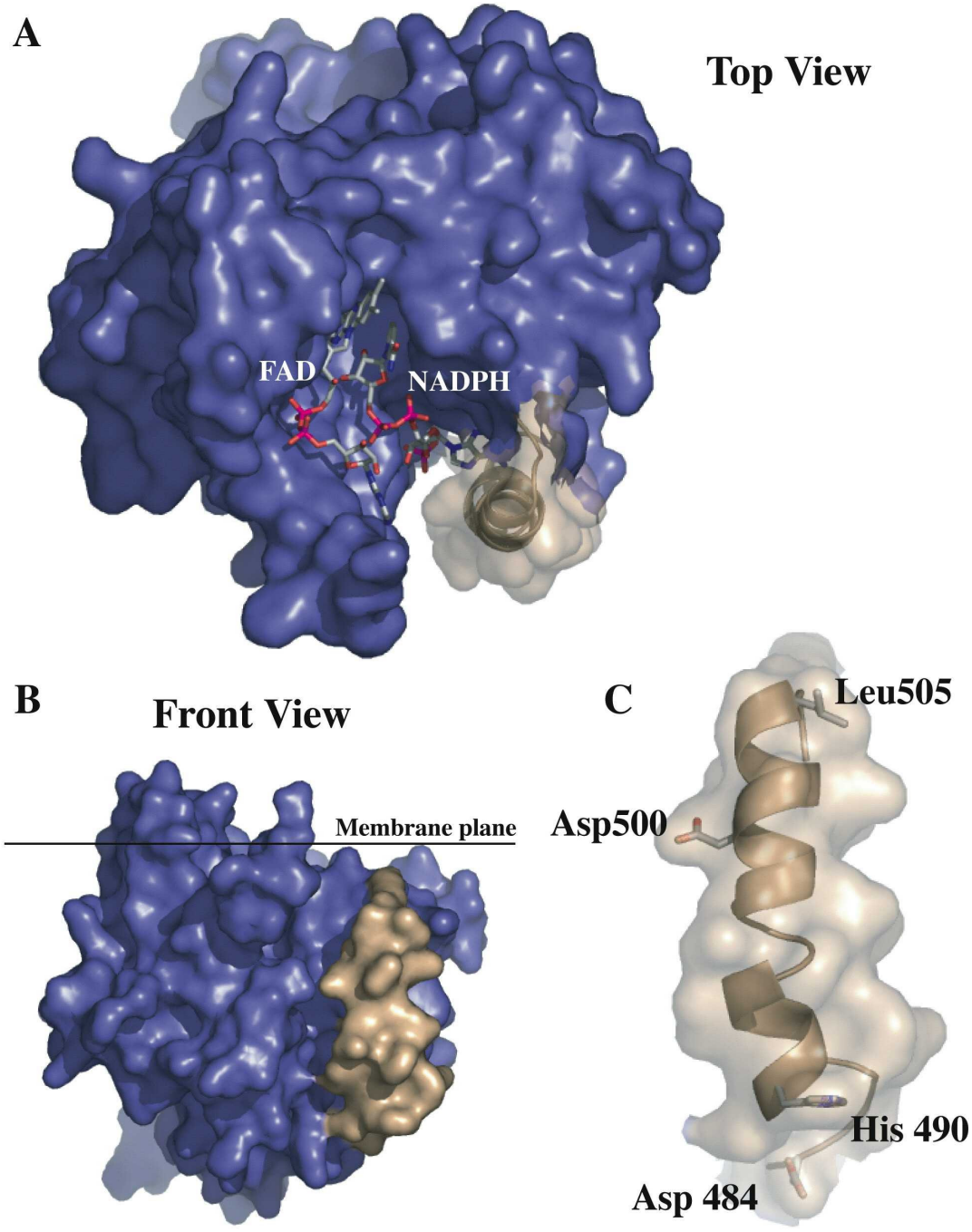
A
Top View
FAD
NADPH
B
Front View
Membrane plane
C
Leu505
Asp500
His 490
Asp 484

Figure 8